ARIEL UNIVERSITY

FACULTY OF NATURAL SCIENCES

Reducing Stress Reactions of Autonomous Vehicles Passengers

A thesis submitted in fulfillment of the requirements for the degree
Master of applied mathematics and computer science
In the Department of Computer Science

By

Fleicher MICHAEL

This work was prepared under the supervision of:

PROF. Azaria AMOS
DR. Musicant OREN

March, 2022

ARIEL UNIVERSITY

FACULTY OF NATURAL SCIENCES

Reducing Stress Reactions of Autonomous Vehicles Passengers

A thesis submitted in fulfillment of the requirements for the degree
Master of applied mathematics and computer science
In the Department of Computer Science

By

Fleicher MICHAEL

This work was prepared under the supervision of:

PROF. Azaria AMOS
DR. Musicant OREN

March, 2022

Dedicated to my beloved wife and life partner, which act as motivational fuel for solving my life's challenges, as much as for conducting this research . . .

Acknowledgements

I would like to thank Ariel University for the fellowship which support me while conducting my research.

I would also like to thank AMOS azaria and OREN musicant for investing their time in this research, shared their experience and patiently supported.

The research presented in this paper was (partially) funded by the The Israeli Smart Transportation Research Center (ISTRC)

Contents

Ariel University

Abstract

Faculty of Natural Sciences
Department of Computer Science

Master

Reducing Stress Reactions of Autonomous Vehicles Passengers

by Fleicher MICHAEL

Objective:
1. To study the relationship between physiological indices and kinematic indices during driving events in an autonomous vehicle (AV) ride.
2. To study how to taking into account the passenger's stress level while planning motion and controlling AV's, and the effect on the driving performance.
Background: Especially for automated vehicles, if driving style becomes stressful, passengers may choose to avoid using AV technology. The AV driving style can be characterized by kinematic parameters of velocity, acceleration, and jerk. Passenger stress is often manifested in changes to physiological indices, such as heart rate and skin conductance. However, little attention was given to associating changes in physiological indices with changes in autonomous vehicle kinematics, and how acting upon these insights can effect to better design AVs behaviour?.
Method: We study database [6] of twenty volunteers participated in a field experiment in which the AV driving style was adjusted to allow a variety of velocity and acceleration values. We used several linear regression models to study the relationship between the intensities of the AVs' kinematic events (braking, accelerating, and turning) characterized by velocity, acceleration and jerk, and changes in heart rate, heart rate variability, and skin conductance. Furthermore, we assimilated stress estimators inside a vehicle motion control and obtained an autonomous vehicle that considers its passenger's stress reactions.
Results:
1. All physiological indices were associated with driving intensity. Utilizing simple regression models and only a few kinematic variables, we explained 65% of the variability in passengers' heart rate in braking events and 55% of the variability in heart rate is accelerating events.
2. The utilization of result 1 in a motion control planning algorithm that considers the passenger's responses in its actions. Such "passenger-aware driving" seems safer while keeping a smaller distance from surrounding objects, and the learning process of such algorithms can be more effective than standard agents.
Application: Associating AV kinematics with physiological indices related to short-term driving events may guide the AV designers on better adjusting the AV driving style to avoid stressful experiences for the passengers.

Keywords: stress, effort, physiology, motor control, kinematics, autonomous vehicle

List of Figures

List of Tables

List of Abbreviations

SCR	**S**kin **C**onductance **R**esponse
AV	**A**utonomous **V**ehicle
ADAS	**A**dvanced **D**river **A**ssistance **S**ystems
SEA	**S**ociety of **A**utomotive **E**ngineers
SEA+3	SEA level 3 and above
ANS	**A**utonomic **N**ervous **S**ystem
SNS	**S**ympathetic autonomic **N**ervous **S**ystem
PSNS	**P**arasympathetic autonomic **N**ervous **S**ystem
SCL	**S**kin **C**onductance **L**evel
EDA	**E**lectrodermal **A**ctivity
GSR	**G**alvanic **S**kin **R**esponse
HR	**H**eart **R**ate
HRV	**H**eart **R**ate **V**ariability
ECG	**E**lectrocardiogram
BPM	**B**eats **P**er **M**inutes
DTW	**D**ynamic **T**ime **W**arping
RL	**R**einforcement **L**earning
NPC	**N**on **P**layer **C**haracters
CAN bus	**C**ontroller **A**rea **N**etwork
LGSVL-SIM	**LG S**ilicon **V**alley **SIM**ulator

Chapter 1

Introduction

In a world where 90% of all motor vehicle accidents are caused by some type of human error [35] the search for an automated solution for driving a vehicle seems inevitable. But there are safety issues that are wildly publicized, and recent accidents have initiated concerns regarding the drivers' understanding and capability of using this technology safely [39]. Therefore, it is quite plausible that individuals would be very concerned when they attempt an autonomous vehicle ride. Despite the rapidly progressing race for fully autonomous vehicles, few trust-related barriers prevent universal acceptance of such technology, and recent studies show that 65-75% of American drivers are afraid to ride in a fully self-driving vehicle [7]. [13] claims that passenger-vehicle interactions will promote confidence, control, and a sense of safety for the people operating AVs and propose a system architecture that links self-driving functionality with visual, audible, and other communication with passengers. It is very likely that people's concerns could be mitigated or on the contrary, enhanced depending on the driving style of the vehicle. People have different driving styles. Today, AVs are driving by pre-defined driving styles, which keeps safety compliance under top priority but pays no attention to preserving or imitating the passengers' preferred driving style. For example, while some people prefer to drive in a more assertive and offensive style, some people prefer a much more defensive and calm experience [10]. A study exploring the preferability of driving styles between various drivers [45] suggested a new approach to exploring preferred driving styles for autonomous vehicles through simulation of autonomous driving in real road conditions. It showed that a defensive driving style was preferred, and there were variations among participants related to their driving style. Furthermore, a recent survey [8] suggests that people are open to more sophisticated vehicle technology and ready to embrace new technology, especially if it makes driving safer. Therefore, to promote acceptance of such technology it is necessary to monitor users' reactions to it as a means to adjust the driving style to their reactions. A review paper [9] proposed autonomous passenger awareness factors and compared them with traditional driving-comfort measures, which eventually linked drivers' preferred driving style to their comfort during driving. The comfort feeling during can be represented by the lack of stress, and several studies tried to decrease the passenger's stress during driving: [32] proposed a neural network-driven based solution to learning driving-induced stress patterns and correlating it with statistical, structural, and time-frequency changes observed in recorded bio-signals. They envisaged that such a driver-centric safety system would help save precious lives by providing fast and credible real-time alerts to drivers and their coupled cars. [48] presented a system where a simple and low-complexity classification algorithm is used to identify a person's stress while driving a car.

The primary missing factor in the results of the above studies is that there is much difference between manually driving and sitting inside an AV as a passenger.

Those differences are probably related to AV passengers' lack of cognitive load during autonomous riding and can dramatically affect their comfort/stress experience. The current study aims to link the autonomous driving style expressed by kinetic-characteristics to the passengers' stress-related response and utilize this linkage in a vehicle control system that takes the passenger stress-state into account.

Autonomous Vehicles
Autonomous Vehicle **(AV)** is a wide range of advanced driver assistance systems **(ADAS)**, which mainly focus on the ability of the car to perform tasks that in the past used to be performed by the drivers, such as steering the wheel, control the gas and brake pedals, and navigate the car safely to its destination. Those abilities are achievable mainly thanks to the ability to sense the environment, whether it is indoors or outdoor. The level of the AV is defined by the SAE levels of driving automation [28], which is ranged between 1-5, while the levels 3 and above **(SAE 3+)** mention that the passengers do not take place in the driving task and the vehicle can drive itself under all conditions [33]. The last two decades witnessed tremendous progress in the area of autonomous driving technology, which significantly improves active safety and energy-saving performances of the vehicle [35]. Currently, due to limitations and high costs of available sensors, most commercial vehicles only include Level 1 to Level 2 autonomy, which requires constant driver attention and control. The autonomous features in these vehicles generally consist of emergency braking, blind-spot detection, and/or lane-keeping. Nonetheless, Level 3 autonomous features are available in the Tesla Model S and Model 3.

Human's Stress reactions
The Autonomic nervous system (**ANS**), which innervates the smooth musculature of all organs, the heart, and the glands, mediates the internal milieu's neuronal regulation. The actions of this system, as its name implies, are, in general, not under direct voluntary control [21]. In this study we focused on reactions related to the Sympathetic autonomic nervous system **(SNS)**, which also known as the "fight or flight" system. SNS increases energy expenditure and inhibits digestion. The following changes take place on activation of the sympathetic nervous system [19]: Heart rate and cardiac muscle contractility increase, the ciliary muscle relaxes, and the pupil becomes dilated for the betterment of far vision, bronchodilation of the lungs, decreased urine output, relaxation of the detrusor muscle of the bladder and contraction of urethral sphincters, increased secretions from sweat glands, increased blood flow to muscles because of relaxation of arterioles, dilation of coronary arteries, constriction of large arteries and large veins, increased metabolism, increased glucose production and mobilization by the liver, suppression of the immune system. During stress, the activity of the SNS is changed globally, leading to an increase in cardiovascular function [14] and therefore, in this research, the focus is on responses that occur by the SNS, which best describes situations where AV's passengers feel some threat during driving sessions.

Below are the most significant SNS responses analyzed in this research:

Skin conductance level (SCL) : The change in skin conductance, also known as the electrodermal response **(EDA)**, or in its older terminology as galvanic skin response **(GSR)**, is the phenomenon that the skin momentarily becomes a better conductor of electricity when either external or internal stimuli occur that are physiologically arousing [22]. GSR can be decomposed to 2 major components - skin conductance

level (SCL), a slowly changing measure of tonic physiological activity, and skin conductance response (SCR), quick bursts of elevated conductance levels resembling peaks. SCL has a strong correlation to emotional stress [3] and especially when it comes to stress during driving [49].

Heart rate (HR) and heart rate variability (HRV) : Human HR is measured through Electrocardiogram **(ECG)**, while HRV is the physiological phenomenon of variation in the time interval between heartbeats. While The SNS activity leads to an increase in HR (e.g., during sports exercise), the Parasympathetic autonomic nervous system **(PSNS)** activity induces a lower HR (e.g., during sleep). The two circuits are constantly interacting, and this interaction is reflected in HRV. HRV, therefore, provides a measure to express the activity of the ANS and may consequently provide a measure for stress [38]. In addition, previous studies suggest that HR and HRV recordings may have the potential to measure stress levels [38].

Reinforcement Learning
Reinforcement learning enables the model to learn to perform the task through trial and error. Reinforcement learning can be modeled as a Markov decision process, formally described as a tuple (S, A, P, R), where S denotes the state space, A represents the action space of possible actions, P denotes the state transition probability model, and R represents the reward function. At each time-step the agent observes a set of states s_t, takes an action a_t from possible actions A, and then the environment transitions according to P. The agent then observes a new set of states s_{t+1} and receives a reward r_t. The target of the agent is to learn a policy $\pi(s_t, a_t)$ mapping observations to actions such that the accumulated rewards are maximized. Therefore, the agent can learn from its actions through interactions with the environment and receives an estimate of its performance through the reward function. The advantage of this approach is that no labeled data sets are required, and behavior that generalizes well to new scenarios can be learned through reinforcement learning. The downside of reinforcement learning is its low sample efficiency [42], which means converging to an optimal policy can be slow, requiring time-intensive simulations or costly real-world training [37].

1.1 Related Work

This section reviews a researches related to physiological reactions while riding a vehicle, how to mitigate such reactions, and previous studied which considered the passenger's experience while controlling an AV.

Stress and physiological responses
State anxiety, defined by [34] as a complex emotional response to a perceived threat, characterized by feelings of tension and heightened autonomic nervous system activity. [47] measured participant's HR and found that mean pulse rate was moderately correlated with the anxiety level and claimed that wearable sensors have the potential to be used for assessing anxiety level objectively and unobtrusively to facilitate mental-stress related studies. [38] explored measures of HR and HRV with an imposed stressful situation and suggested that HR and HRV change with a mental task, and that HR and HRV recordings may have the potential to measure stress levels. [43] claimed that "Stress is triggered by something called stressor. A stressor is a stimulus initiating or sparking changes. In general, stressor is classified further

into internal stressor and external stressor." they manged to detect an individual's level of stress by measuring heart rate, blood pressure, and Galvanic Skin Response (GSR). [31] used GSR to objectively evaluate stress and arousal levels, and showed that GSR readings significantly increase when task's cognitive load level increases.

Driving as an external stressor
On [11] the researchers present methods for collecting and analyzing physiological data during real-world driving tasks to determine a driver's relative stress level (during manual driving). HR, HRV, and SCL were recorded continuously alongside other stress-related measurements while drivers followed a set route through open roads. Data from 24 drives of at least 50-min duration were collected for analysis. The data were analyzed in two ways. Analysis I used features from 5-min intervals of data during the rest, highway, and city driving conditions to distinguish three levels of driver stress with an accuracy of over 97% across multiple drivers and driving days. Analysis II compared continuous features, calculated at 1-s intervals throughout the entire drive, with a metric of observable stressors created by independent coders from videotapes. The results show that skin conductivity and heart rate metrics are most closely correlated with driver stress levels for most drivers studied. These findings indicate that physiological signals can provide a metric of driver stress in future cars capable of physiological monitoring. Such a metric could be used to help manage noncritical in-vehicle information systems. Another work [6], measured physiological signals (HR, eye-movement patterns, and Skin conductance level (SCL)) and self-reported comfort and anxiety levels from passengers in an autonomous vehicle followed by correlation of passengers' response with driving style parameters, including acceleration, jerk (the third derivative of position), and dynamic object distance (proximity of the AV to other objects, like other cars), as well as four events: following a lead vehicle; stopping at a sign; passing a vehicle; a tight turn. The study took place on a closed track in an autonomous vehicle. The results managed to explain the passengers' responses to various driving style in a physical autonomous vehicle, and how the kinetic characteristics of the ride effects on those responses. the presence and proximity of a lead vehicle not only raised the level of all measured physiological responses but also exaggerated the existing effect of the longitudinal acceleration and jerk parameters. SCL response was also found to be a significant predictor of passenger comfort and anxiety. Using multiple independent events to isolate different driving style parameters demonstrates a method to control and analyze such parameters in future studies.

Stress due to kinetic indices during driving
[15] used skin conductance responses (SCRs) to measure learner, novice and experienced drivers' psycho-physiological responses to the development of driving hazards and found that experienced drivers were twice as likely to produce an SCR to developing hazards as novice drivers and three times as likely when compared with learner drivers. [4] explored whether slight differences in real-world driving task demands could be discriminated by electrodermal response (EDR). The likelihood of EDR and, whenever present, its duration were both correlated with workload as represented by the deceleration demand. A higher base travel speed and the unexpected demand of the emergency braking situation impacted EDR, thus attesting higher workload level. EDR explained why stopping the vehicle from 50 km/h and slowing down from 80 to 50 km/h was of similar strain. The results further demonstrate that EDR measures can be successfully employed to discriminate multiple levels of workload. [24] made a field experiment and manipulated braking demands

such as pre-braking speed and and the target speed for braking (30 km/h, a complete stop, or responding to an impending collision) and found that all SCL, HR and HRV were associated with deceleration intensity, and especially when $|g| > 0.5$, and suggested that SCL, HR and HRV can mirror the mental workload elicited by varying braking intensities.

Vehicle control

Early autonomous vehicle systems relied on accurate sensory data, utilizing multi-sensor setups and expensive sensors such as LIDAR to provide accurate environment perception. Control of these autonomous vehicles was handled via rule-based controllers, where the developers hand-tuned the parameters after simulation and field testing [18],[25]. Recently, deep learning has gained attention due to the numerous state-of-the-art results it has achieved in fields such as image classification and speech recognition [16],[12],[36]. This has led to increasing use of deep learning in autonomous vehicle applications, including planning and decision making [30], [41]; perception [1],[40]; as well as mapping and localisation [17]. In early works towards vehicle control through deep learning, xia2016control introduced an autonomous driving system based on Q-learning combined with learning from the experience of a professional driver. The reward value of the professional driver's strategy and the Q-value learned through the Q-learning method were combined in the pre-training phase to improve convergence speed during training. A filtered experience replay stores a limited number of episodes and allows the elimination of poor experimental rounds from memory, improving convergence on a control strategy. The proposed Deep Q-learning with filtered experiences (DQFE) approach was compared to a naive neural fitted Q-iteration (NFQ) riedmiller2005neural algorithm without pre-training by an experienced driver. During training, it was shown that the DQFE approach reduced the training time by 71.2% for the 300 training episodes. Moreover, during 50 tests on a competition track, the proposed approach completed the track 49 times, compared to only 33 with NFQ. Additionally, DQFE performed better in terms of the mean distance from the center of the track. Therefore, adding filtered experience replay improved the speed of convergence as well as the performance of the algorithm. Comparing two neural networks for lane-keeping systems, [29] investigated the effects of discretized and continuous actions. Two approaches, DQN and a Deep Deterministic Actor-Critic (DDAC) algorithm were evaluated in a TORCS simulator [44]. In the two networks developed by the authors, the DQN could only output discretized values (steer, gear, brake, and acceleration), while the DDAC supports continuous action values. The DDAC consisted of two networks; an Actor-Network, a neural network responsible for taking actions based on perceived states, and the Critic Network, which criticizes the value of the action taken. The experimental results showed that the DQN algorithm suffered in performance since it cannot support continuous actions or state spaces. The DQN algorithm is suitable for continuous (input) states. However, it still requires discrete actions since it finds the action that maximizes the action-value function. In this study, we explored different approach for using DQN, which discretely changes continuous outputs in order to be able to output high range of discrete values without increasing the dimensionality and complexity of the network.

Current study

Based on the reviewed literature, it appears that there would be a need to facilitate the acceptance of autonomous vehicles. The empirical literature also presents previous work that linked driving style to stress via physiological markers. In the current

study, we would explore different methods for relating kinetic indices to passengers' stress during riding AV and facilitate them into stress predictors. We then would try to adjust those predictors to be suitable for integration onto a DQN vehicle control architecture which itself adjusted to be used as a passenger-aware vehicle control system.

Chapter 2

Methodology

This section describes the processes of this study and its two primary outcomes:

1.Association of physiological indices with driving intensity and Prediction of stress-related responses of AV passengers based on kinematic indices.
2. The utilization of outcome 1 in a motion control planning algorithm that considers the passenger's responses in its operation.

2.1 the relation between kinetic indices to the stress reactions of AV's passengers

The data used in this study were collected elsewhere (Dillen et al. 2020 [6]). We describe the data in brief: The study was conducted on a closed and circular test track in Waterloo, Ontario, Canada, and involved using an AV, a "normal" vehicle, and human participants. The AV, a Lincoln MKZ hybrid research platform developed at the University of Waterloo [5] to reach Level 3 autonomy. The AV was fitted with an array of sensors, including a Novatel inertial measurement unit (IMU), Novatel Global Positioning System (GPS), Velodyne Light-Detection-and-Ranging (LIDAR). The usage of the GPS and IMU allowed the researchers to collect the raw velocity, acceleration, and Jerk (the third derivative of position) with respect to both longitudinal and lateral directions during the entire experiment. The LIDAR allowed the researchers to measure the distance to surrounding objects like "normal" vehicles deliberately parked alongside the road. The motion planning algorithm [46] onboard the vehicle used the sensor information to select a trajectory in accordance with the intended driving style and the current environmental constraints. Two of the participant's physiological response sources were measured: GSR, HR (and HRV). A Shimmer3+ device was used to measure GSR (500Hz sample rate) and obtain a PPG signal for HR and HRV.
Using this experiment's data allowed us to investigate the relation between the kinetic indices (including the distance to surrounding vehicles) and the stress-related physiological responses.

Preprocessing of acceleration and physiological data: To filter out long-term drifts in acceleration values, we analysed the raw acceleration signal minus its moving median (30sec). We then subtracted the moving median from the filtered data. Then the acceleration data (lateral and longitudinal) was subjected to outlier detection and removal according to the 1.5IQR method. A sample above the third quartile + 1.5* interquartile range or below the first quartile-1.5* interquartile range was removed.

Detection of kinematic and physiological events: The kinetic of the vehicle applies forces on the vehicle, and there are translating functions to forces on the passengers. One way to estimate the linkage between the forces applied to the passengers and their physiological response is to look at the time-series data Dillen et al. [6] provided such analysis. They report that the presence and proximity of a lead vehicle not only raised the level of all measured physiological responses but also exaggerated the existing effect of the longitudinal acceleration and jerk parameters. Skin response was also found to be a significant predictor of passenger comfort and anxiety. Our approach is different and does not assume that the kinematic forces and physiological responses occur simultaneously. To illustrate, we plotted ($Figure 2.1$) the longitudinal acceleration (orange line) and the Skin Conductance Level (SCL) versus measurement number (measured in 500[Hz]). The figure presents three acceleration events: Braking, with peak deceleration at 21.72K measurement, Accelerating with peak acceleration at 21.77K measurement, and Braking with peak 21.9k measurement. The letters S and E signify the start and end of each kinematic (and physiological) event identified in the data. A kinematic event (acceleration state 1 or -1 for throttle and brake events, respectively) begins when the acceleration is higher than 0.1[$\frac{m}{sec^2}$] or lower than -1.1[$\frac{m}{sec^2}$].There are also events (that we call Skin Conductance Responses - SCR), with peaks at times: 21.7K measurement, 21.75K measurement, and 21.88K measurement.

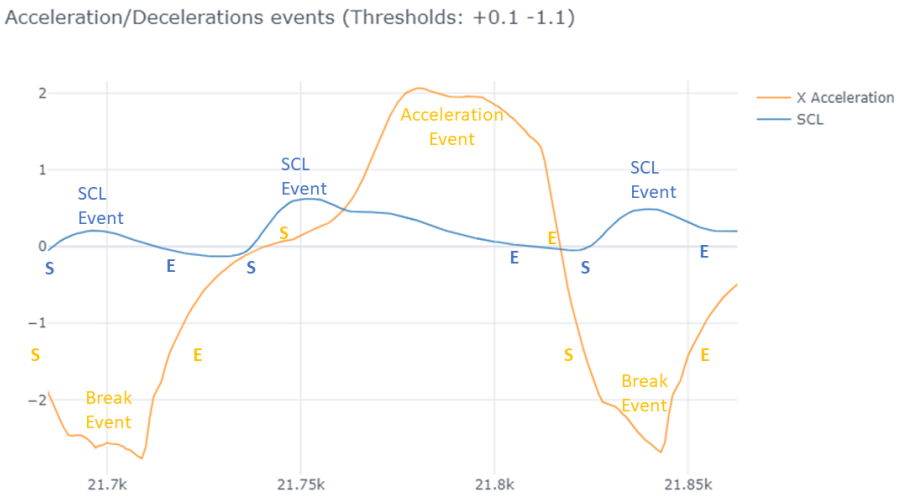

FIGURE 2.1: Acceleration, and SCL response during some trials of the experiment.
X axis represents measurement number (sampled in 10Hz)
Orange line represents actual acceleration [$\frac{m}{sec^2}$]
Blue line represents SCL response
Thresholds of -1.1, +0.1 [$\frac{m}{sec^2}$] defines the acceleration/braking event type

The time of the peaks of the kinematic events is not perfectly synchronized with those of the physiological event, suggesting that the psychological event can appear before the kinematic event (proactive response) or after (reactive). For example, in [15], SCRs began before a hazardous event onset reflecting the driver's (in their case) ability to anticipate hazards. Here too, the peak in the physiological event (at time 21.75k measurement) preceded the peak of the acceleration event. The peak of the braking events and their corresponding SCR are almost aligned.

While the analysis of the correlation between two time-series (physiological and kinematic) requires an assumption about the time lag between the kinematic time series and the physiological time series, analyzing data per event may allow more flexibility: the correlation uses the pairs of peaks in the kinematic and the physiological data in the overlapping events even if the peaks did not occur at the same time.
Many other thresholds were explored using grid search. we tested different thresholds for both negative and positive accelerations, in the longitudinal and lateral direction. For each threshold, we calculated linear regression to relate between the kinetic characteristics of the driving, to the passenger's HR. Then we choose the threshold which facilitated the highest R^2 score between kinetic indices to the passenger's stress response. This procedure yielded 418 braking events, 486 acceleration events, 692 right turn, and 0 left turn events. Naturally, due to the circular structure of the driving track, only right turns were made in this experiment.
We calculated several indices based on the data accumulated between the event onset and end per each of the kinematic events. The indices are maximal instantaneous HR and SCL responses.

Regression models for the physiological response: Using various linear regression models, we analyzed the statistical linkage between the intensity characteristics of various kinematic events, braking, acceleration, and turning. The simplest regression model we used, contains combination of 1 or more of the variables in the following equation :

$$P = \beta_0 + \beta_1 V + \beta_2 V^2 + \beta_3 A_{longitudinal} + \beta_4 J_{Longitudinal} + \beta_5 A_{Lateral} + \beta_6 J_{Lateral} + \epsilon$$

Where P is the dependent variable representing the physiological response that we recorded during the period of the kinematic event (from S to E - see $Figure$ 2.1 and text above it) which in our case, can be represent as HR or SCL. We fitted the model several times with a different physiological index as the dependent variable. V represents the maximal velocity of the vehicle during the kinematic event, $A_{Longitudinal}$ ($J_{Longitudinal}$) is the maximal acceleration (Jerk) in the longitudinal direction. The magnitude of these indices will be high during braking and accelerating events. $A_{Lateral}$ ($J_{Lateral}$) represents the maximal acceleration (Jerk) in the lateral direction. Thus the magnitude of these indices is high during turning events. ϵ represents the error

2.2 Vehicle control

This section outlines the regression models' assimilation into an AV motion control planning algorithm called "passenger-aware agent". The motion control of a vehicle can be broadly divided into two tasks - lateral and longitudinal motion; the steering of the vehicle controls the lateral motion of the vehicle, while longitudinal motion is controlled by manipulating the gas and brake pedals of the vehicle. Lateral control systems aim to control the vehicle's position on the lane and carry out other lateral actions such as lane changes or collision avoidance maneuvers. In the deep learning domain, this is typically achieved by capturing the environment using the images from onboard cameras as the input to the neural network. Longitudinal control manages the vehicle's acceleration such that it maintains the desirable velocity on

the road, keeps a safe distance from the preceding vehicle, and avoids rear-end collisions. While lateral control is typically achieved through vision, longitudinal control relies on relative velocity and distance measurements to the preceding/following vehicles. Data set from Dillen et al. [6] experiment was used to develop several SCL and HR predictors, and their performance will be described in the results section. Due to its relatively high coefficient of determination ($R_{squared}$), the heart rate response was used as the predicted human stress indicator in this section. Due to its relatively small amount of sub-estimators and parameters, the $BaggingRegressor$ model [20] is used as the primary predictor used in this section. In order to predict the passenger's heart rate as a response to the vehicle kinetics state, the following variables were used as the predictor's input:

$$[V, A_{Longitudinal}, A_{Lateral}, J_{Longitudinal}, J_{Lateral}, D_{Longitudinal}, D_{Lateral}, N_{steps}, T, B, A, N_T, N_B, N_A]$$

Where,
V - Represents the vehicle velocity $[\frac{m}{sec}]$
$A_{Longitudinal}$ ($J_{Longitudinal}$) - Acceleration $[\frac{m}{sec^2}]$ (Jerk $[\frac{m}{sec^3}]$) in the longitudinal direction
$A_{Lateral}$ ($J_{Lateral}$) - Acceleration (Jerk) in the lateral direction
$D_{Longitudinal}$($D_{Lateral}$) - Distance from surrounding objects, which are vehicles in our case, in the longitudinal (lateral) direction
N_{steps} - Number of steps made by the agent since the beginning of the current driving session
T (B) [A] - A binary flag which sets to 1 if turning (braking) [acceleration] event occur, and 0 otherwise
N_T (N_B) [N_A] - Number of turning (braking) [acceleration] events occurred since the beginning of the current driving session

In order to design a vehicle control mechanism, we used an API of LGSVL-SIM [27] simulator as a training environment, which facilitated the same conditions as conducted on Dillen et al. [6], such as maximum acceleration and velocity thresholds and nearby NPC's (non-player characters). The vehicle used in the simulator uses several sensors to feed the observation space, control space, reward function, and the heart rate predictor.

Segmentation camera sensor: An image obtained from a front camera on the vehicle's roof as input and transformed using a segmentation algorithm. Objects in the image are colored corresponding to their tag: Ego - the AV (Black), NPC (Blue), Road (Purple), Horizon (White).

Controller Area Network (CAN bus) sensor: Sends data about the vehicle chassis. The data includes: Velocity[m/s], Angular velocity[rad/sec] , Longitudinal Acceleration [m/sec^2], Angular Acceleration[rad/sec^2], Lateral Acceleration [m/sec^2], Longitudinal Jerk[m/sec^3], Lateral Jerk[m/sec^3].

Observation space: Contains data retrieved from the Simulator's sensors. Include the current image and the last three images obtained from the segmentation camera sensor. The observation space also includes data from CAN bus sensor.

Control State: Represents the vehicle's current throttle [%], Brake [%], Steering [+-%] states.

Action space: Contains the following nine combinations of using the gas/brake pedals and the steering wheel:
no action, throttle, brake, throttle+right, throttle+left, brake+right, brake+left, right, left. Before every step, the agent chooses an action from the action space. every chosen action is increasing/decreasing/resets the current Control state in the following form:
The throttle pedal increases its previous state by 5% if the actions throttle, throttle + right, throttle + left is chosen and drops back to 0% for any other action chosen. The brake pedal is increasing its previous state by 5% if the actions brake, brake + right, brake + left is chosen, and drops back to 0% for any other action chosen.
The steering wheel increases (decreases) by 5% if the actions right, throttle + right, brake + right (left, throttle + left, brake + left) action is chosen and keeps the same for any other action chosen.

Reward Function: After each step, the agent receives a reward according to the results of its action. The reward function uses information about the vehicle location, and while the vehicle's position is inside the road, the reward function calculates the following variables:
Distance traveled: The euclidean distance from the current to the last step's position.
Passenger factor: A value which describes the level of which the passenger's reaction exceed some stress threshold and calculates as follows: $(HR_{predicted}/HR_{threshold})^2$ if $HR_{predicted} >= HR_{threshold}$. 0 otherwise. While $HR_{predicted}$ represents the HR predicted by the $BaggingRegressor$ model using the current steps kinetic information, and $HR_{threshold}$ represents the threshold which, if passed, indicates that the passenger has some level of stress. In our case, the HR threshold is set to 90[BPM].
delay penalty: a value which increases itself in every step. We used the delay penalty to "punish" the agent for standing still and encourage the agent to move along the road. The delay penalty calculates as follows: $0.05 * (step_{number} - 1)/1000$

As a result, the reward calculates as follows:
reward = distance traveled - passenger factor - delay penalty

If the vehicle location is outside of the road or if the vehicle collided with another vehicle or any obstacle, the reward function resets the current driving session and signals the environment to begin a new one.
In order to compare a passenger-aware agent to a standard agent (which controls the vehicle's throttle and steering without taking into count the passenger's stress level), we compared two similar agents, while the only difference between them is the passenger factor element in the reward function. Thus, the standard agent's reward function is equal to: reward = distance traveled - delay penalty

Architecture: Using DQN architecture [23], a vehicle control agent was then optimized to implement the heart rate prediction model and compare the so-called "passenger aware agent" driving performance to the standard "no passenger awareness" vehicle control agent.

The DQN uses the observation space as an input and, as an output, returns one element from the action space as an action. $Figure$ 2.2 describes the entire DQN network structure. As an agent takes actions and moves through an environment, it learns to map the observed state of the environment to an action. An agent will choose an action in a given state based on a "Q-value" - a weighted reward based

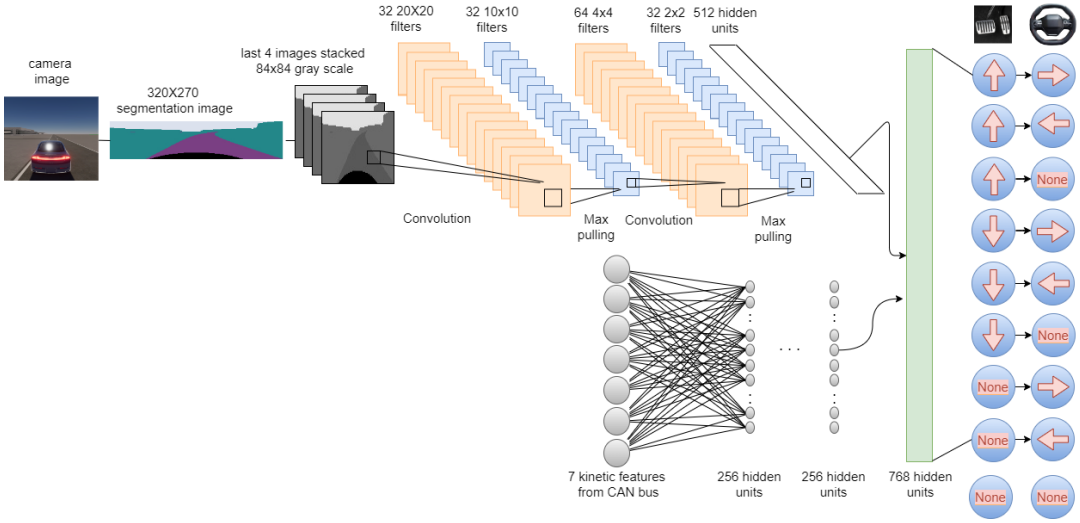

FIGURE 2.2: Visualization of the DQN architecture we used. the network receives 4 images and kinetic features as and input and outputs one action from the action space for controlling the vehicles wheel and brake/throttle pedals.

on the expected highest long-term reward. A Q-Learning Agent learns to perform its task such that the recommended action maximizes the potential future rewards. This method is considered an "Off-Policy" method, meaning its Q values are updated assuming that the best action was chosen, even if the best action was not chosen. This network learns an approximation of the Q-table - a mapping between the states and actions that an agent will take. For every state, we will have nine actions that can be taken. The environment provides the state, and the action is chosen by selecting the larger of the nine Q-values predicted in the output layer. Our network is built as a combination of two different neural networks merged to decide one action as an output. The upper part (in $Figure$ 2.1) is a network that can process images data (4 stacked images in our case) and use convolution layers to understand features in the image, such as the road and NPCs. The upper network receives 4 84x84 gray images and then performs a transformation on two convolution layers while using max pulling in between. As an output, the upper network outputs a dense layer of 512 units. This output will merge with the lower network's output.
The lower network receives the kinetic information of the vehicle from the CAN bus sensor and uses it as an input. The input is then processed through two dense layers of 256 units. The last layer of 256 units are merged with the upper network's last layer of 512 units to a single 768 dense layer, which then outputs 9 Q-values. Later on, the agent chooses the action in which its representative q-values have the highest values. For detailed information about this process, visit our Github page.

Chapter 3

Results

This chapter describes in detail the results of two primary outcomes:
1. Prediction of stress-related reactions to kinetic indices on AV passengers.
2. The utilization of outcome 1 in a motion control planning algorithm that considers the passenger's responses in its actions.

3.1 Prediction of stress-related reactions to kinetic indices on AV passengers

Linear regression: The mathematic relation between kinetic indices and AV passengers' stress reactions (HR) is described below. We used linear regression to produce a straightforward function that inputs several vehicle kinetics and estimates the passenger's HR. Unfortunately, SCL estimation had poor accuracy and correlation and was thus excluded from this section. In order to achieve better results, we performed linear regression only to 1 type of event each time, and therefore, we have functions that estimate the passenger's HR according to the type of event. Using the methods described in chapter 2, we separated the Dillen et al. [6] data into three types of events: turning, acceleration, and deceleration.
below are the coefficients of different regression models to estimate HR using kinetic variables. each model uses different combination of kinetic variables. Tables 3.2-3.4 variables represents the following:

$V_x =$ Longitudinal velocity $[\frac{m}{sec}]$
$a_x =$ Longitudinal Acceleration $[\frac{m}{sec^2}]$
$a_y =$ Lateral Acceleration $[\frac{m}{sec^2}]$
$J_x =$ Longitudinal Jerk $[\frac{m}{sec^3}]$
$J_y =$ Lateral Jerk $[\frac{m}{sec^3}]$

And where each event defined by the values of a_x and a_y as follows:

Event type	Condition
Brake	$a_x < -1.1$ and $-0.1 < a_y < 0.1$
Acceleration	$a_x > 0.1$ and $-0.1 < a_y < 0.1$
Turn	$a_y > 0.1$ or $a_y < -0.1$

TABLE 3.1: The definition of and the thresholds for longitudinal and lateral accelerations.

Turning events occur whenever lateral acceleration magnitude exceeds some threshold, while in this case, there is no importance to the current longitudinal

acceleration value. Acceleration/Braking events occur whenever there is no turning event and while the longitudinal acceleration exceeds some threshold. This setting is made this way because when lateral acceleration occurs, it indicates that the event is "turning", even when longitudinal acceleration occurs. Thus, we should check whether the event turns or throttles whenever the longitudinal acceleration occurs.

Coefficients of different HR estimation models (during acceleration events)							
	Model 1	Model 2	Model 3	Model 4	Model 5	Model 6	Model 7
R^2	0.05	0.57 *	-0.13	0.5 *	0.56 *	0.5 *	0.56 *
$RMSE$	25.11	16.74	27.41	18.11	17.01	18.11	16.83
V_x		0.35		0.43	0.82	2.23	0.58
V_x^2			-0.03		0.11		
a_x	1.64			1.63	1.86	156.34	1.94
a_y							0.004
J_x						-6.95	
J_y							
$Constant$	70.11	72.83	112.57	70.11	66.08	41.48	64.93

TABLE 3.2: The coefficient of each HR estimation models during acceleration events. each column represents a certain model and its variable's coefficients. R^2 stands for R squared score, and RMSE stands for root mean squared error. models with high R^2 are marked with $*$.

Coefficients of different HR estimation models (during deceleration events)							
	Model 1	Model 2	Model 3	Model 4	Model 5	Model 6	Model 7
R^2	0.19	0.62 *	-0.12	0.65 *	0.62 *	0.66 *	0.63 *
$RMSE$	21.38	14.59	25.33	13.98	14.55	13.92	13.97
V_x		0.77		0.7	1.18		0.82
V_x^2			-0.0032		0.11	15.58	
a_x	1.1			1.12	2.91	10.08	1.64
a_y							0.034
J_x						-1.08	
J_y							
$Constant$	72.86	68.49	97.36	73.8	59.83	56.43	69.3

TABLE 3.3: The coefficient of each HR estimation models during deceleration events. each column represents a certain model and its variable's coefficients. R^2 stands for R squared score, and RMSE stands for root mean squared error. models with high R^2 are marked with $*$.

Coefficients of different HR estimation models (during turning events)							
	Model 1	Model 2	Model 3	Model 4	Model 5	Model 6	Model 7
R^2	0.09	0.62 *	-0.02	0.64 *	0.64 *	0.65 *	0.66 *
$RMSE$	24.71	15.86	26.34	15.6	15.47	15.51	13.98
V_x		2.44		1.72	8.24	10.51	
V_x^2			0.07		0.7		1.44
a_x	1.1			2.44	3.94	14.25	2.01
a_y						-30.54	1.96
J_x						4.47	
J_y						15.53	
$Constant$	72.66	92.66	103.2	79.66	56.4	28.93	58.46

TABLE 3.4: The coefficient of each HR estimation models during turning events. each column represents a certain model and its variable's coefficients. R^2 stands for R squared score, and RMSE stands for root mean squared error. models with high R^2 are marked with $*$.

Our results show that most of the unexplained variance in passenger's HR can be explained by equation 3.1, as long as this regression tries to estimate the HR of the same participants whose data is published here. However, to achieve a more robust and generalized regression, there is a need for a larger dataset. If examining only the constant presented in $Tables$ 3.2-3.4, one can mistakenly assume that while the vehicle is standing without any movement, the HR estimated is the value of each model constant variable, but in our case, standing without movement is not belong to any of the mentioned turning, acceleration, braking events.

Non-linear regressors:
In order to better explain the variance in the passenger's stress response, we processed some non-linear regressors on the entire dataset, measured with a 500Hz sample rate (after performing the pre-processing described in chapter 2.1). In order to achieve higher accuracy, we assumed that using the features extracted in chapter 2.1 would result a higher accuracy in estimating the passenger's stress responses.
Thus, we trained several regressors for estimating the passenger's HR or SCR using the below parameters as inputs:

$$V, A_{Longitudinal}, A_{Lateral}, J_{Longitudinal}, J_{Lateral}, D_{Longitudinal}, D_{Lateral}, N_{steps}, T, B, A, N_T, N_B, N_A$$

Where,

V	Vehicle velocity $[\frac{m}{sec}]$
$A_{Longitudinal}$	Acceleration $[\frac{m}{sec^2}]$ in the longitudinal direction
$J_{Longitudinal}$	Jerk $[\frac{m}{sec^3}]$ in the longitudinal direction
$D_{Longitudinal}$	Distance from surrounding vehicles in the longitudinal direction $[meter]$
$D_{Lateral}$	Distance from surrounding vehicles in the lateral direction $[meter]$
N_{steps}	Sum of steps made since the beginning of the current session
T	Binary flag which sets to 1 if turning event occur, and 0 otherwise
B	Binary flag which sets to 1 if braking event occur, and 0 otherwise
A	Binary flag which sets to 1 if acceleration event occur, and 0 otherwise
N_T	Sum of turning events occurred since the beginning of the current session
N_B	Sum of braking events occurred since the beginning of the current session
N_A	Sum of acceleration events occurred since the beginning of the current session

Furthermore, the accuracy of each model is described below:

	HR		SCL	
Model	R^2	RMSE	R^2	RMSE
RandomForestRegressor	0.8086	0.0721	0.7330	0.0952
ExtraTreesRegressor	0.8018	0.0723	0.7764	0.0890
BaggingRegressor	0.7786	0.0784	0.7069	0.1043

TABLE 3.5: Coefficient of determination R^2 and root mean squared error RMSE of different models for estimating passengers' HR and SCL during riding AV.

Table 3.5 shows that the ability to estimate passengers' stress levels during AV riding exists and the error of such estimations is less than 1 BPM for HR estimations. However, there is high importance to take into account that those estimations will estimate accurately only on the passengers who participated in Dillen et al. [6] experiments. For the generalization of such estimators, there is a need for data from a higher population. In our research, those results were enough for implementing the $BaggingResgressor$ in an AV motion planning and control algorithm, as described in the next section.

Discussion:
The results presented in this section connect AV passengers' stress reactions to the ride's kinetic characteristics. Some key points to remember while considering those results are that all of those estimations were trained on a significantly low population of 20 people and cannot be generalized to the external population. Furthermore, the data set that this study used to develop the HR estimations upon, contains driving sessions of significantly low speed (of 0-34 $[kmh]$) and, therefore, cannot be used to estimate HR while driving in higher speeds, and especially not using the linear models presented here. In order to address those limitations, a further study that will measure higher popularity, and a higher range of speeds, can support the validation of the current study's results.

3.2 Motion control planning algorithm which considers the passenger's responses in its actions

After both agents where trained, we summarized the kinetics characteristics of the passenger-aware agent during a 500 episodes of driving. the results are below:

	Units	Max	Min	Mean	Std
Forward Velocity	m/s	11.61	-0.018	7.25	3.85
Lateral Acceleration	m/s^2	3.93	-4.103	0.01	0.6
Forward Acceleration	m/s^2	3.33	-4.02	-0.15	0.79
Lateral Jerk	m/s^3	2.17	-2.28	-0.00016	0.22
Forward Jerk	m/s^3	3.38	-3.74	-0.007	0.35

TABLE 3.6: Summary statistics of kinetic variables while driving 500 episodes using the passenger-aware agent

After training both passenger-aware and standard agents five times each, we compared the distance traveled by each during an episode. The episode represents a driving session, and while training our algorithms, the agents made thousands of episodes. In *Figure* 3.1, we plotted the distance traveled by the agents during each episode to compare their performance.

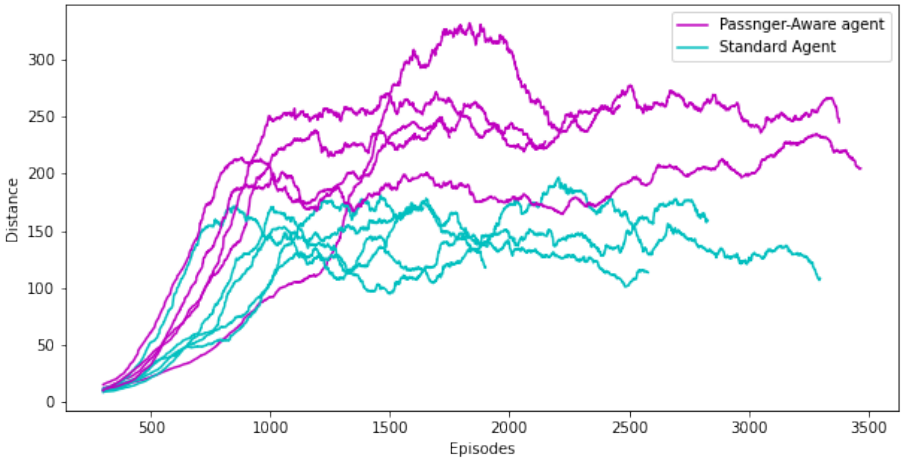

FIGURE 3.1: Distance traveled vs. the number of episodes colored by agent type. each agent made five different learning sessions

In *Figure* 3.1, if each agent is examined separately, we can see a significant difference between the agent's performance from one learning session to another. This phenomenon can be explained by the fact that before each step, the agent chooses its actions in some level of randomness. The use of epsilon greedy [26] in order to deal with the exploration-exploitation dilemma [2] during the training process can explain this randomness and possibly explain the temporary high distance traveled on one of the passenger-aware agent's trials (around 1500-2000 episodes). *Figure* 3.1's significant outcome is the existence of a mechanism that can learn how to avoid increasing the passenger's stress reactions and control and plan the motion of a vehicle - all at the same time. Furthermore, while comparing the performance of our passenger-aware agent to a standard agent (which is the same algorithm with just one difference - the passenger's factor calculated in the algorithm's reward function, as described in section 2), we can see that the learning process of passenger-aware agent converges to a higher distance of driving without resets the episodes. Those results can even tell that it is recommended to implement the passenger factor in other algorithm's reward functions to gain higher performance.

We then analyzed how each agent interacts with other vehicles during the ride, and

mainly focused on the proximity to other vehicles during an episode. We collected all the events where the agent's vehicle passed near a surrounding vehicle, and for each event, we took the minimum euclidean distance between those two vehicles. *Figure* 3.2 presents the results:

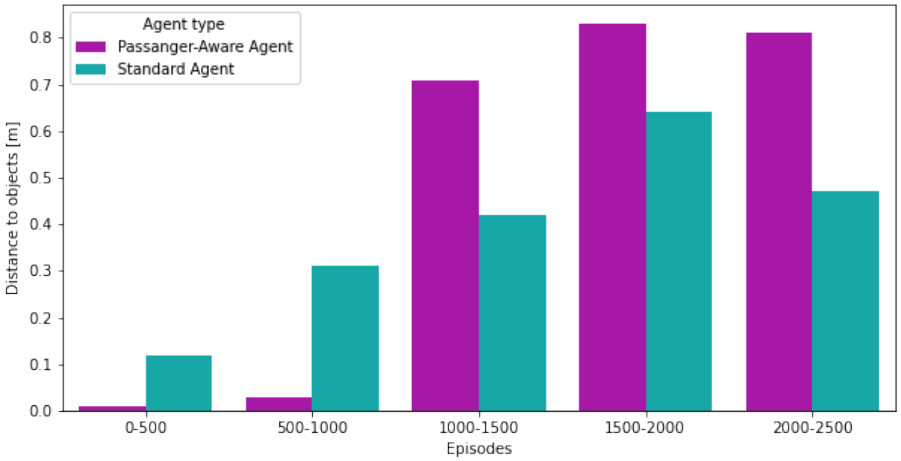

FIGURE 3.2: We calculated the minimum distance between the agent's vehicle and the surrounding vehicle for each agent type in every episode. Then we calculated the average across 500 episodes for every learning session (5 in total) and calculated the average.

By *Figure* 3.2, we can learn that as the time passed, the passenger-aware agent learned to keep its distance from surrounding vehicles, significantly compared to the standard agent. Furthermore, we assume the agent acts in such way to avoid triggering stress reactions in passengers, similar to [6], which found that the presence and proximity of a lead vehicle raised the level of all measured physiological responses. As a result, such behavior can be interpreted as a bit safer. The primary outcome of these results is that eventually, and as expected, driving with a passenger awareness can also contribute to a safer driving strategy, especially when comparing the two above control agents' distance keeping abilities.

We then inspected how each one of the episodes ended during the training. In our environment, an episode ends if one of the following occurs: the vehicle went off the road, the vehicle collides with another vehicle, and the session reaches the maximum steps defined for each episode (in our case is 1000 steps). We focused on situations where episodes ended due to collisions.

Figure 3.3 shows the average collusion around every 500 episodes during all five learning sessions of each agent. We did so to observe how each agent was able to sense the surroundings and avoid collisions.

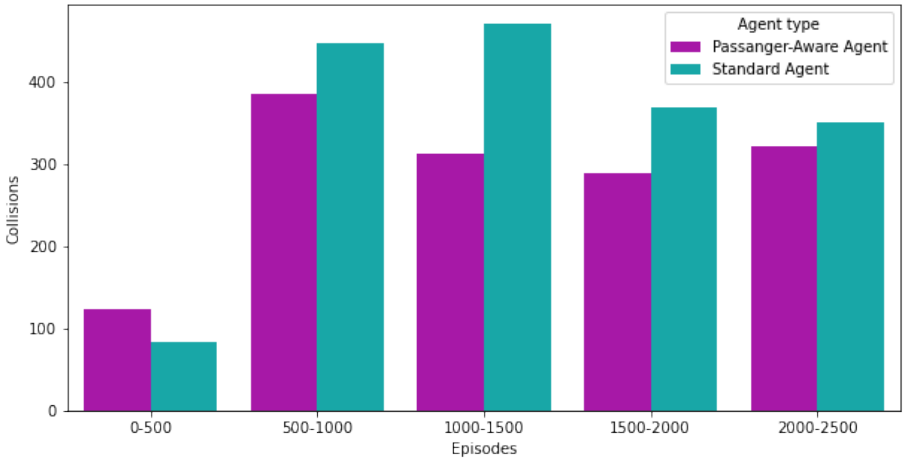

FIGURE 3.3: We summed the collisions of every 500 episodes for each agent and computed the average value around five learning sessions.

Figure 3.3 shows that the passenger-aware agent eventually managed to collide with other vehicles less than the standard agent. A possible reason for those results can be explained by *Figure* 3.2 outcomes which is, as expected, the idea that driving with higher distance keeping can contribute to collision avoidance.

Discussion:
The results presented in this section support the usage of the passenger factor we used here in experiments evolving physical AV due to the fewer collisions rate during training. However, to proceed with on-road testing, there should be a usage of control agents with a much lower collision rate (around zero), which is measured by much more simulations compared to only five as we did. A key point to remember while considering this study's results is that even though the passenger factor was reliable by presenting high accuracy of HR estimation, it was calculated by significantly small population size and thus, cannot be generalized to a higher or external population other than its population. Therefore, those results need to be addressed only as proof of the feasibility of such an AV control strategy. Another way to handle the disadvantages of those results is to examine how such a passenger-aware agent can learn its HR estimation upon individual users, and by then, to learn how to provide personal driving experiences custom-made to individuals instead of to some population.

Bibliography

[1] Rodrigo Benenson et al. "Ten years of pedestrian detection, what have we learned?" In: *European Conference on Computer Vision*. Springer. 2014, pp. 613–627.

[2] Oded Berger-Tal et al. "The exploration-exploitation dilemma: a multidisciplinary framework". In: *PloS one* 9.4 (2014), e95693.

[3] Wolfram Boucsein. *Electrodermal activity*. Springer Science & Business Media, 2012.

[4] C Collet, E Salvia, and C Petit-Boulanger. "Measuring workload with electrodermal activity during common braking actions". In: *Ergonomics* 57.6 (2014), pp. 886–896.

[5] Ian Colwell. "Runtime restriction of the operational design domain: A safety concept for automated vehicles". MA thesis. University of Waterloo, 2018.

[6] Nicole Dillen et al. "Keep calm and ride along: passenger comfort and anxiety as physiological responses to autonomous driving styles". In: *Proceedings of the 2020 CHI Conference on Human Factors in Computing Systems*. 2020, pp. 1–13.

[7] Ellen Edmonds. *AAA: Three in Four Americans Remain Afraid of Fully Self-Driving Vehicles*. https://newsroom.aaa.com/2019/03/americans-fear-self-driving-cars-survey/. 2019.

[8] Ellen Edmonds. *AAA: Today's Vehicle Technology Must Walk So Self-Driving Cars Can Run*. https://newsroom.aaa.com/2021/02/aaa-todays-vehicle-technology-must-walk-so-self-driving-cars-can-run/. 2021.

[9] Mohamed Elbanhawi, Milan Simic, and Reza Jazar. "In the passenger seat: investigating ride comfort measures in autonomous cars". In: *IEEE Intelligent transportation systems magazine* 7.3 (2015), pp. 4–17.

[10] Davina J French et al. "Decision-making style, driving style, and self-reported involvement in road traffic accidents". In: *Ergonomics* 36.6 (1993), pp. 627–644.

[11] Jennifer A Healey and Rosalind W Picard. "Detecting stress during real-world driving tasks using physiological sensors". In: *IEEE Transactions on intelligent transportation systems* 6.2 (2005), pp. 156–166.

[12] Geoffrey Hinton et al. "Deep neural networks for acoustic modeling in speech recognition: The shared views of four research groups". In: *IEEE Signal processing magazine* 29.6 (2012), pp. 82–97.

[13] Adam Jordan Jack Weast Matt Yurdana. *a matter of trust: how smart design can accelerate automated vehicle adoption*. https://www.intel.com/content/dam/www/public/us/en/documents/white-papers/trust-autonomous-white-paper-secure.pdf. 2019.

[14] Arthur SP Jansen et al. "Central command neurons of the sympathetic nervous system: basis of the fight-or-flight response". In: *Science* 270.5236 (1995), pp. 644–646.

[15] Neale Kinnear et al. "Understanding how drivers learn to anticipate risk on the road: A laboratory experiment of affective anticipation of road hazards". In: *Accident Analysis & Prevention* 50 (2013), pp. 1025–1033.

[16] Alex Krizhevsky, Ilya Sutskever, and Geoffrey E Hinton. "Imagenet classification with deep convolutional neural networks". In: *Advances in neural information processing systems* 25 (2012).

[17] Sampo Kuutti et al. "A survey of the state-of-the-art localization techniques and their potentials for autonomous vehicle applications". In: *IEEE Internet of Things Journal* 5.2 (2018), pp. 829–846.

[18] Tuan Le-Anh and MBM De Koster. "A review of design and control of automated guided vehicle systems". In: *European Journal of Operational Research* 171.1 (2006), pp. 1–23.

[19] Tyler LeBouef, Zachary Yaker, and Lacey Whited. "Physiology, Autonomic Nervous System". In: *StatPearls [Internet]* (2020).

[20] Gilles Louppe and Pierre Geurts. "Ensembles on random patches". In: *Joint European Conference on Machine Learning and Knowledge Discovery in Databases*. Springer. 2012, pp. 346–361.

[21] Laurie Kelly McCorry. "Physiology of the autonomic nervous system". In: *American journal of pharmaceutical education* 71.4 (2007).

[22] *MIT - What is the skin conductance response?* https://www.media.mit.edu/galvactivator/faq.html.

[23] Volodymyr Mnih et al. "Human-level control through deep reinforcement learning". In: *nature* 518.7540 (2015), pp. 529–533.

[24] Oren Musicant et al. "Relationship between kinematic and physiological indices during braking events of different intensities". In: *Human factors* 60.3 (2018), pp. 415–427.

[25] Michel Pasquier, Chai Quek, and Mary Toh. "Fuzzylot: a novel self-organising fuzzy-neural rule-based pilot system for automated vehicles". In: *Neural networks* 14.8 (2001), pp. 1099–1112.

[26] Michael Rawson and Radu Balan. "Convergence Guarantees for Deep Epsilon Greedy Policy Learning". In: *arXiv preprint arXiv:2112.03376* (2021).

[27] Guodong Rong et al. "Lgsvl simulator: A high fidelity simulator for autonomous driving". In: *2020 IEEE 23rd International conference on intelligent transportation systems (ITSC)*. IEEE. 2020, pp. 1–6.

[28] *SAE International Releases Updated Visual Chart for Its "Levels of Driving Automation" Standard for Self-Driving Vehicles*. https://www.sae.org/news/press-room/2018/12/sae-international-releases-updated-visual-chart-for-its-%E2%80%9Clevels-of-driving-automation%E2%80%9D-standard-for-self-driving-vehicles.

[29] Ahmad El Sallab et al. "End-to-end deep reinforcement learning for lane keeping assist". In: *arXiv preprint arXiv:1612.04340* (2016).

[30] Wilko Schwarting, Javier Alonso-Mora, and Daniela Rus. "Planning and decision-making for autonomous vehicles". In: *Annual Review of Control, Robotics, and Autonomous Systems* 1.1 (2018), pp. 187–210.

[31] Yu Shi et al. "Galvanic skin response (GSR) as an index of cognitive load". In: *CHI'07 extended abstracts on Human factors in computing systems*. 2007, pp. 2651–2656.

[32] Rajiv Ranjan Singh, Sailesh Conjeti, and Rahul Banerjee. "A comparative evaluation of neural network classifiers for stress level analysis of automotive drivers using physiological signals". In: *Biomedical Signal Processing and Control* 8.6 (2013), pp. 740–754.

[33] *Society of Automotive Engineers*. https://www.sae.org/.

[34] Charles D Spielberger. "Theory and research on anxiety; in Anxiety and behavior". In: *Spielbergered* (1966), pp. 3–22.

[35] NHTSA's National Center for Statistics and Analysis. *2016 Fatal Motor Vehicle Crashes: Overview*. https://crashstats.nhtsa.dot.gov/Api/Public/ViewPublication/812456.

[36] Ilya Sutskever, Oriol Vinyals, and Quoc V Le. "Sequence to sequence learning with neural networks". In: *Advances in neural information processing systems* 27 (2014).

[37] RS Sutton. *andA. G. Barto,"Reinforcement learningan introduction"*. 1998.

[38] Joachim Taelman et al. "Influence of mental stress on heart rate and heart rate variability". In: *4th European conference of the international federation for medical and biological engineering*. Springer. 2009, pp. 1366–1369.

[39] *Tesla update halts automatic steering if driver inattentive*. https://phys.org/news/2016-09-tesla-halts-automatic-driver-inattentive.html. (Accessed on 21/06/2021).

[40] Jessica Van Brummelen et al. "Autonomous vehicle perception: The technology of today and tomorrow". In: *Transportation research part C: emerging technologies* 89 (2018), pp. 384–406.

[41] Sandor M Veres et al. "Autonomous vehicle control systems—a review of decision making". In: *Proceedings of the Institution of Mechanical Engineers, Part I: Journal of Systems and Control Engineering* 225.2 (2011), pp. 155–195.

[42] Ziyu Wang et al. "Sample efficient actor-critic with experience replay". In: *arXiv preprint arXiv:1611.01224* (2016).

[43] Nurdina Widanti et al. "Stress level detection using heart rate, blood pressure, and GSR and stress therapy by utilizing infrared". In: *2015 International Conference on Industrial Instrumentation and Control (ICIC)*. Ieee. 2015, pp. 275–279.

[44] Bernhard Wymann et al. "Torcs, the open racing car simulator". In: *Software available at http://torcs. sourceforge. net* 4.6 (2000), p. 2.

[45] Nidzamuddin Md Yusof et al. "The exploration of autonomous vehicle driving styles: preferred longitudinal, lateral, and vertical accelerations". In: *Proceedings of the 8th international conference on automotive user interfaces and interactive vehicular applications*. 2016, pp. 245–252.

[46] Yu Zhang et al. "Hybrid trajectory planning for autonomous driving in highly constrained environments". In: *IEEE Access* 6 (2018), pp. 32800–32819.

[47] Yali Zheng et al. "Unobtrusive and multimodal wearable sensing to quantify anxiety". In: *IEEE Sensors Journal* 16.10 (2016), pp. 3689–3696.

[48] Pamela Zontone et al. "Low-complexity classification algorithm to identify drivers' stress using electrodermal activity (EDA) measurements". In: *The World Thematic Conference-Biomedical Engineering and Computational Intelligence*. Springer. 2018, pp. 25–33.

[49] Pamela Zontone et al. “Stress detection through electrodermal activity (EDA) and electrocardiogram (ECG) analysis in car drivers”. In: *2019 27th European Signal Processing Conference (EUSIPCO)*. IEEE. 2019, pp. 1–5.

אוניברסיטת אריאל בשומרון

הפקולטה ל: מדעי הטבע

הורדת לחץ לנוסעים ברכב אוטונומי

חיבור זה מוגש כחלק מהדרישות לקבלת התואר "מוסמך האוניברסיטה" (M.Sc.)

במחלקה למדעי המחשב

על ידי:

מיכאל פליישר

העבודה הוכנה בהדרכתו\הדרכתם של

פרופ' עמוס עזריה , דוק' אורן מוזיקאנט

28.4.22 כ"ז ניסן, התשפ"ב

אוניברסיטת אריאל בשומרון

הפקולטה ל: מדעי הטבע

הורדת לחץ לנוסעים ברכב אוטונומי

חיבור זה מוגש כחלק מהדרישות לקבלת התואר "מוסמך האוניברסיטה" (M.Sc.)

במחלקה למדעי המחשב

על ידי:

מיכאל פליישר

העבודה הוכנה בהדרכתו\הדרכתם של

פרופ' עמוס עזריה , דוק' אורן מוזיקאנט

28.4.22 כ"ז ניסן, התשפ"ב